NUMERICAL ANALYSIS OF TURBULENT CONVECTIF FLOW IN HEAT EXCHANGERS PROVIDED WITH THE BAFFLES

SAIM Rachid, e-mail: saimrachid@mail.univ-tlemcen.dz
ABBOUDI Said, e-mail: said.abboudi@utbm.fr
FMSTO-ST, UMR CNRS 6174, Département CREST, UTBM, Site de Sévenans- 90100 - France

BENYOUCEF Boumedienne, e-mail : b_benyoucef@mail.univ-tlemcen.dz
Unité de Recherche des Matériaux et Energies Renouvelables (URMER)-Faculté des Sciences –Université Abou Bakr Belkaid-BP 119- Tlemcen-13000- Algérie

Abstract. *This study presents the numerical predictions on the turbulent fluid flow and heat transfer characteristics for rectangular channel provided with the transverse baffles . The turbulent governing equations, based on the K -ε model, are solved by the finite volumes method. The velocity and pressure terms of momentum equations are solved by SIMPLE (Semi- Implicit method for pressure-linked equation) algorithm. The mean velocity profiles, the velocity and temperature fields as well as the Nusselt number distribution are presented for a typical case and for the representative value of Reynolds Nember.*

Keywords: *Finite volume method, turbulent flow, forced convection, baffles, rectangular channel*

1. INTRODUCTION

Forced convection in complex geometries receives considerable attention due to its importance in many engineering applications and has been the subject of interest for many researchers. Some of these include the energy conversion systems found in Somme design of nuclear reactor, heat exchangers, solar collectors and cooling of industrial machines and electronic components.

Considerable work has been done, in recent years, on the investigations of the flow and heat transfer processes at the shell-side are of special interest in order to improve the accuracy of prediction of heat exchangers performances. Somme works are of particular interest in the improvement and the prediction of the flows around baffles. These studies are devised as well experimental and numerical techniques.

An extensive experimental studies of turbulent flow past baffles in heat exchangers has been performed by Demartini et al (2004), Roetzel and Lee (1993), Berner et al. (1984) and Habib et al. (1994). They investigated the heat transfer and turbulent flow over perpendicular baffles of different heights. The heat flux was uniform in both upper and lower walls. The experiments are focused on the influence of Reynolds number and baffles height, on the local and global heat transfer coefficient, and pressure drop measurements. Large recirculation regions and velocity gradient were observed behind the baffles.

A numerical analysis was conducted for the laminar forced convection between parallel plates with baffles by Kelkar and Patankar (1987). Results show that the flow is characterized by strong deformations and large recirculation regions. In general, Nusselt number and friction coefficient increase with the Reynolds number.

Chen and Huang (1991) and Webb and Ramadhyani (1985) have been focused their numerical studies on the forced laminar convection in parallel-plate channels with transverse fin arrays. Results show that the flow is characterized by strong deformations and large recirculation regions. In general, Nusselt number and friction coefficient increase with the Reynolds number.

The turbulence models were also investigated by many studies. We can distinguish work from Launder and Spalding (1974) which proposed, for the first time, a model *k-ε* with low Reynolds number (LRN) by presenting functions of attenuation based on the turbulent Reynolds number. Many alternatives of this model were proposed by Versteeg and Malalasekera (1995) with differences on the level of the constants values of the models and formulas of attenuation of these functions.

In this work, a numerical investigation was carried to examine by the K -ε model, the turbulent flow of air and heat transfer in a two-dimensional horizontal plane channel in the presence of rectangular baffles plates.

2. MATHEMATICAL FORMULATION

2.1. Statement of the problem

The geometry of the problem is presented on figure 1. It is about a rectangular conduit provided with two baffles of rectangular form crossed by a steady and turbulent flow of air satisfying the following assumptions: (i) All the physical properties of the fluid and of the solid are considered constant, (ii) The flow enters at constant temperature T_{in} and with uniform velocity profile U_{in}, (iii) plate walls are maintained at constant temperature T_w, (VI) Model of turbulence adopted is the Low Reynolds Number (LRN).

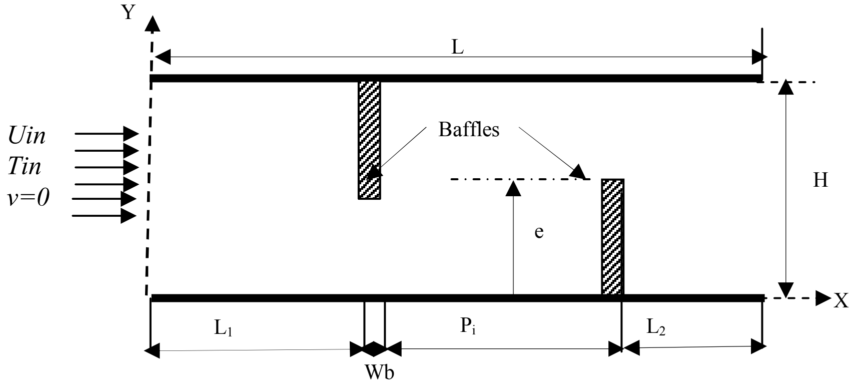

Figure 1. Geometry of the problem

2.2. Governing Equations

Under these conditions, the governing transport equations to be considered are the continuity, momentum and energy equations. A k-ε model is used to account for the effect of turbulence phenomena. Then, the general governing equations can be written in the form as:

$$\frac{\partial}{\partial x}(\rho u\phi)+\frac{\partial}{\partial y}(\rho v\phi)=\frac{\partial}{\partial x}\left[\Gamma_\phi\frac{\partial\phi}{\partial x}\right]+\frac{\partial}{\partial y}\left[\Gamma_\phi\frac{\partial\phi}{\partial y}\right]+S_\phi \qquad (1)$$

Where :

ϕ stands for the dependent variables *u, v, k, T* and *ε.*

u and *v* are local time-averaged velocity in the *x* and *y* directions respectively, T the temperature, k turbulent kinetic energy and ε is the dissipation rate of turbulence energy;

Γ_ϕ and S_ϕ are the corresponding turbulent diffusion coefficient and source term respectively for general variable ϕ.

The equations of the main flow region are summarized in table 1.

Table 1. Summary of equations solved for the main flow region about ϕ and Γ_ϕ.

Equations	ϕ	Γ_ϕ	S_ϕ	
Continuity	*1*	*0*	*0*	(2)
x-momentum	*u*	μ_e	$\frac{\partial p}{\partial x}+\frac{\partial}{\partial x}(\mu_e\frac{\partial u}{\partial x})+\frac{\partial}{\partial y}(\mu_e\frac{\partial v}{\partial x})$	(3)
y-momentum	*v*	μ_e	$\frac{\partial p}{\partial y}+\frac{\partial}{\partial x}(\mu_e\frac{\partial u}{\partial y})+\frac{\partial}{\partial y}(\mu_e\frac{\partial v}{\partial y})$	(4)
Energy	*T*	μ_e/σ_T	*0*	(5)
Turbulent energy	*k*	$\mu_\ell+\mu_t/\sigma_k$	$-\rho.\varepsilon+G$	(6)
Turbulent dissipation	*ε*	$\mu_\ell+\mu_t/\sigma_\varepsilon$	$(C_1G-C_2\rho.\varepsilon)\frac{\varepsilon}{k}$	(7)

Where:

$$G=\mu_t\left\{2.\left(\frac{\partial u}{\partial x}\right)^2+2.\left(\frac{\partial v}{\partial y}\right)^2+\left(\frac{\partial v}{\partial x}+\frac{\partial u}{\partial y}\right)^2\right\} \qquad (8)$$

$$\mu_e=\mu_\ell+\mu_t$$
$$\mu_t=c_\mu\rho K^2/\varepsilon \qquad (9)$$

Where :

μ_ℓ is the laminar viscosity of the air and μ_t is the turbulent viscosity.

ρ is the density of the air, k is the turbulent kinetic energy, ε is the dissipation rate of turbulence energy, ν is the kinematic viscosity.
C_1, C_2, C_μ , σ_k , σ_ε σ_t are the constant values for k-ε turbulence model mentioned in table 2.

The turbulent constants in above equations were adopted in accordance with those Chieng and Launder (1980). They are shown in Table 2. Since the turbulence model employed in this computation is the high Reynolds number form, it is necessary to introduce the ``wall function" approach (Launder and Spalding, 1974) into the normal procedure for turbulence computation for the wall adjacent numerical cells.

Table 2. Turbulent constants in the governing equations.

C_μ	$C_1 = C_3$	C_2	σ_k	σ_ε	σ_t
0.09	1.44	1.92	1	1.3	0.9

The evaluation of the ε in the wall-vicinity region must be treated specially. ε_p is decided as follows:

$$\varepsilon_p = \frac{C_\mu^{3/4} . K_p^{3/2}}{0.4 y_p} \tag{10}$$

y_p is the distance from position P.

According to the wall-function it demands that the first node point p lie in the fully turbulent region, satisfying $11.5 \le y_p^+ \le 400$ ($y_p^+ = y_p c_\mu^{1/4} k_p^{1/2} / \nu$). On the other hand, since there exists great velocity gradient in the near-wall region, very fine grid is needed to obtain accurate computational result. Thus, it is necessary to take non-uniform grid system to divide the computational domain in y-direction. In the study, the first cell neigh boring the wall was kept large enough to meet $y_p^+ \ge 11.5$ .Starting from the second cell the grid changed from fine to coarse gradually, with a relaxing factor equal to 1.07. The non uniform grid in *x* and *y* directions were found to model accurately the fluid flow and heat transfer in this problem. Non uniform grids are taken in both the fluid and baffles regions (was used in both the vertical and the horizontal directions), with 20x15 nodes in each baffle. This grid is highly concentrated close to the baffle to capture high gradient velocity, pressure and temperature. In order to ensure grid independence of the results, a series of tests for non uniform grids were carried out and the choice of the grid distribution (200× 90) is found to be sufficient for the range of Reynolds numbers investigated for the same conditions of the experimental data published by Demartini et al. (2004).

The Reynolds number is defined for hydraulic diameter D_h:

$$Re = \frac{\rho . D_h . U_{in}}{\mu} \tag{11}$$

In the main flow direction the local heat transfer coefficient *h(x)* is calculated as:

$$h(x) = k_t(x) \frac{T_w - T_p(x)}{y_p} . \frac{1}{T_w - T_b(x)} \tag{12}$$

Where k_t is the turbulent thermal conductivity.
The subscript "p" indicates the first inner node from the solid wall.
Considering that the computation is confined in one cycle and the difference between wall temperature T_w and bulk temperature $T_b(x)$.

$$T_b(x) = \frac{\int_A u(x,y) \cdot T(x,y) dA}{\int_A u(x,y) \cdot dA} \tag{13}$$

The cycle-averaged heat transfer coefficient $\bar{h}$ can be calculated by:

$$\bar{h} = \frac{1}{P_i} \int_0^{P_i} h(x) dx \tag{14}$$

The corresponding local and averaged Nusselt numbers are:

$$Nu(x) = \frac{h(x) D_h}{\lambda_f} \tag{15}$$

And

$$\overline{Nu} = \frac{\bar{h} D_h}{\lambda_f} \tag{16}$$

λ_f is the fluid conductivity

2.3. Boundary conditions:

The boundary conditions of the studied problem are summarized in the following table:

Table 3. Boundary conditions.

ϕ	u	v	T	k	ε
Inlet flow	U_{in}	0	T_{in}	$0.005\ U_{in}^2$	$0.1.k_{in}^{3/2}$
Exit flow	$\partial u/\partial x = 0$	$\partial v/\partial x = 0$	$\partial T/\partial x = 0$	$\partial k/\partial x = 0$	$\partial \varepsilon/\partial x = 0$
Wall	0	0	T_w	0	0

Where the Subscripts *in* is used for the inlet of the test section and *w* the wall

3. NUMERICAL SOLUTION

The governing equations describing the flow and heat transfer in this problem associated with the boundary conditions were solved numerically using a finite volume method. SIMPLE algorithm was adopted. The diffusion terms appearing in the transport equations for momentum and turbulence parameters are discretized using second-order central differencing. The Power-Law Differencing Scheme (PLDS) of Patankar (1980) were used to approximating the convection terms. The discretized governing equation is typically solved using the Tri-Diagonal Matrix Algorithm (TDMA).

4. DISCUSION

From the flow field measurements in the previous works of Demartini. et. al. (2004) and Berner. et. al. (1984), it has been presented that the hydraulic periodicity of the air flow was archived in the region after the flow passed over baffles.

For the numerical simulation presented in this work, we based ourselves on the experimental data published by Demartini et al. (2004): *$Pr=0.71$, $Re=10^5$, $T_{in}=20°C$, $U_{in}=7.8 m/s$, $L=0.554$ m, $H=0.146$ m, $e=0.08$ m, $w=0.01$ m, $L_1=0.218$ m, $L_2=0.174$ m, $Pi=0.142$ m, $D_h=0.167$ m et $T_w=100$ °C*. On the numerical level, we used a constant grid with 200 steps in direction OX and 90 in direction (oy).

Where: Pr is the laminar Prandtl number, Re is the Reynolds number, L is the lenght of the channel, His the channel height, e is the baffle height, W_b is the baffle width, L_1 present the distance upstream of the first baffle, L_2 is the distance downstream of the second baffle, Pi is the spacing between the first and second baffle, D_h is the hydraulic diameter, T_w is the wall temperature

The comparison between the numerical and experimental results Demartini et al. (2004), presented on figure 2, for an axial position x=0,525 m, shows a good agreement between the axial mean velocities.

Figure 3 shows that between the two baffles, the flow is characterized by the very high velocities at the lower part of the channel, approaching 255 % of the reference velocity (U_{in}).

The profiles axial of velocity are represented for three axial positions located in the zones upstream and downstream of each baffle, figures 4, 5, 6 and 7. The field of temperature is presented on figure 8, and the rate of transfer of heat, characterized by the number of Nusselt, then given and is shown along the lower wall of the channel are illustrated in fig 9,10 and 11. The local Nusselt number for the lower wall is presented in the Figure 9. As expected, it can be clearly observed that the values of the Nusselt number become higher between the first and the second baffles plate at $Re=1x10^5$, e/H=0.6 and w=0.975H. This may be explained by the fact that the first baffle situated in the free stream causes a very weak clockwise vortex to from forward to the upward lower corner as was discussed elsewhere Korichi, A. and Oufer, L. (2005).

In Figure 10, it is very quite clear that the local Nusselt number profile upstream the first baffle is almost plat in the upper part of the baffle, while in the lower part the flow starts to accelerate toward the gap above the following baffle plate until the exit for second baffle.

Finally, the evolution of the Nusselt number between first and second baffle is presented in the figure 11. The largest variations are found near the tip of the baffle, due to the strong velocity gradient in that region.

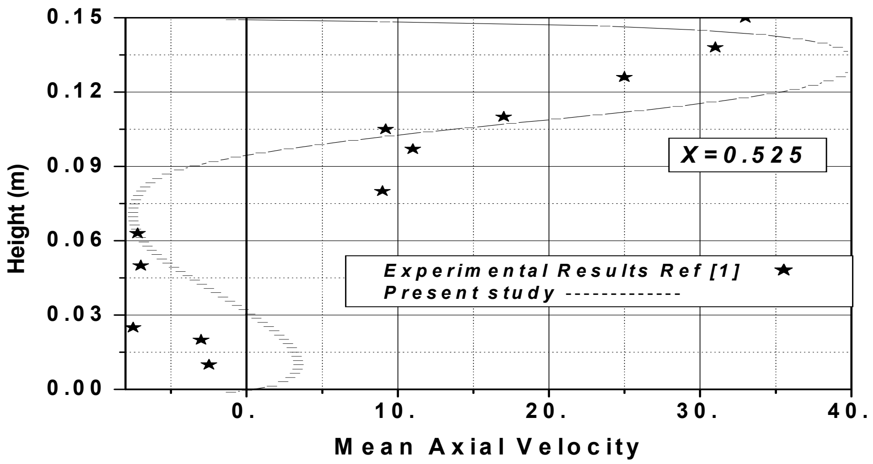

Figure 2. Validation plot of the present numerical simulation with the Experimental results of Demartini, L. C et al (2004)

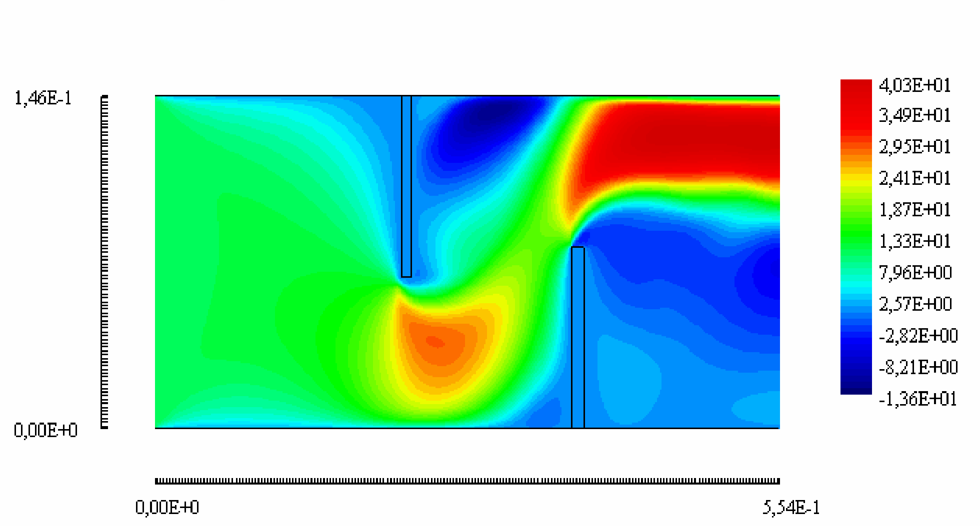

Figure 3. Axial Velocity field distribution. Flow in from left to right. Velocity value in m/s

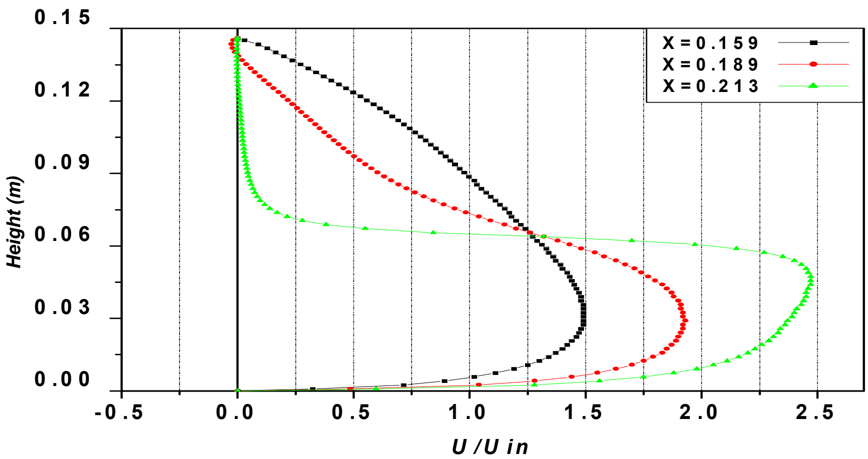

Figure 4. Velocity profiles upstream of the first baffle plate

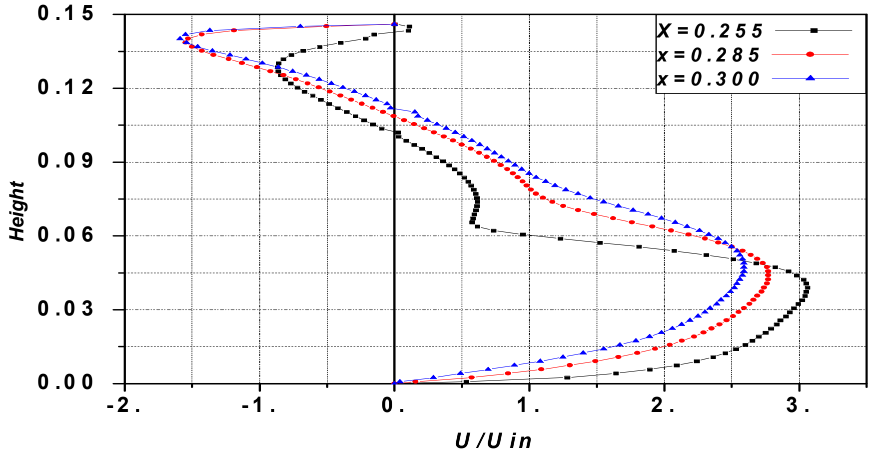

Figure 5. Velocity profiles between the first and the second baffle plates

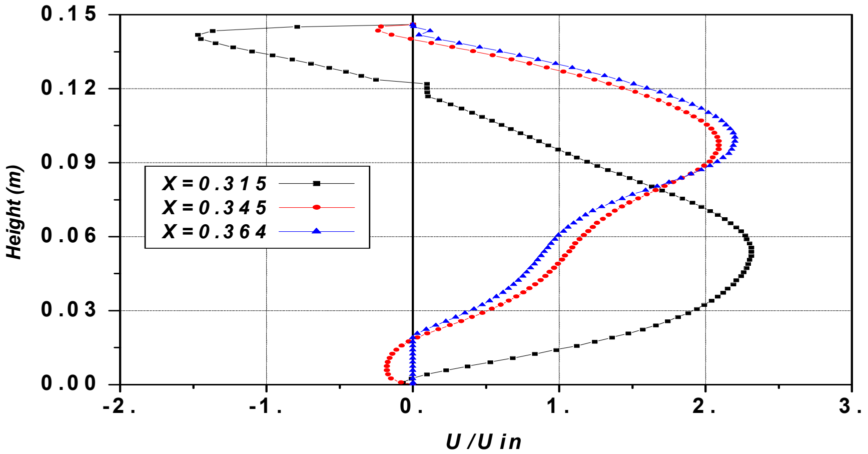

Figure 6. Velocity profiles upstream of the second baffle plate

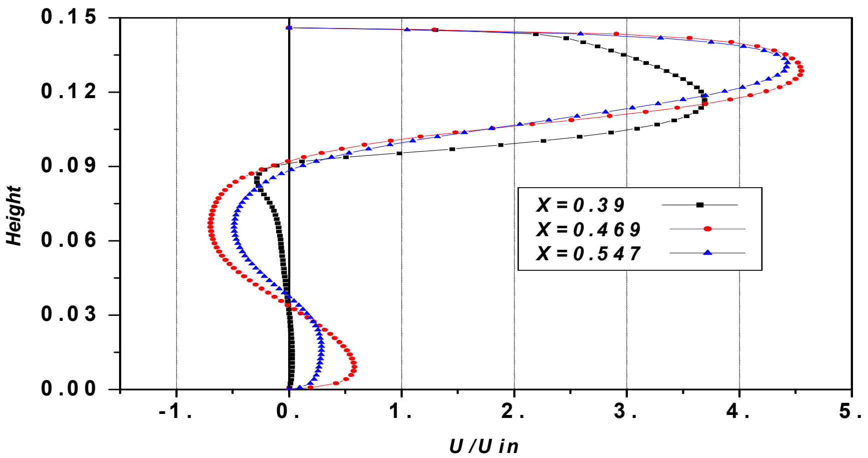

Figure 7. Velocity profiles downstream of the second baffle plate

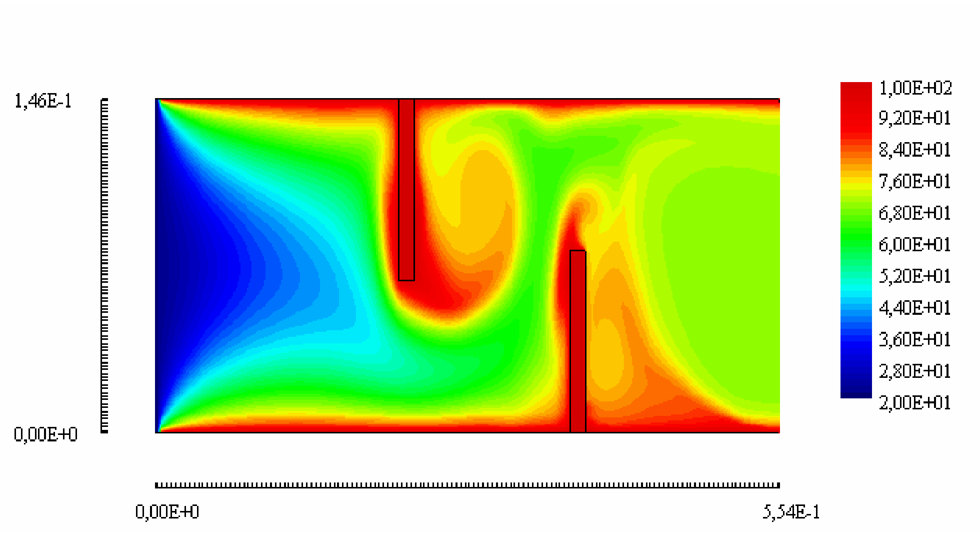

Figure 8. Temperature distribution in the symmetry plane of the 2D baffles. Temperature value in °C

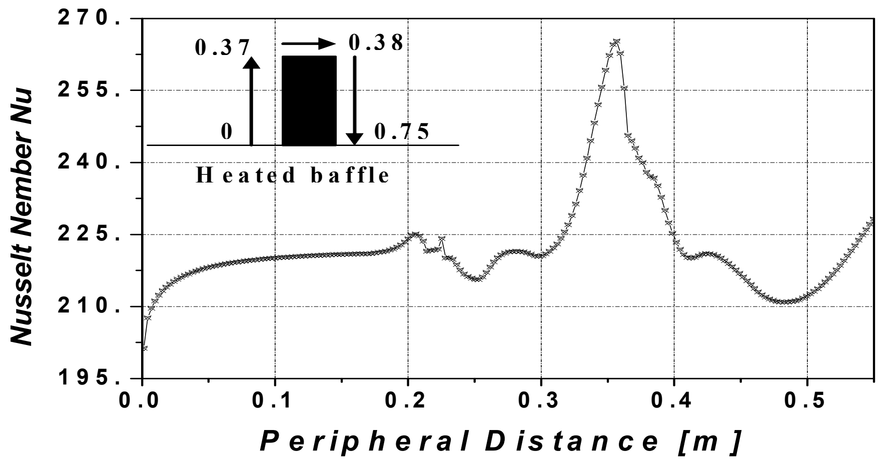

Figure 9. Distribution of the Nusselt number around the second baffle.

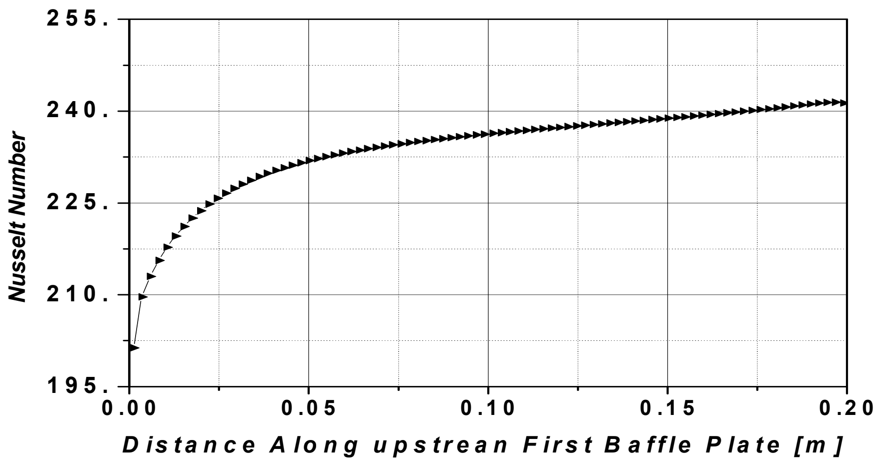

Figure 10. Local Nusselt number distribution upstream the first baffle

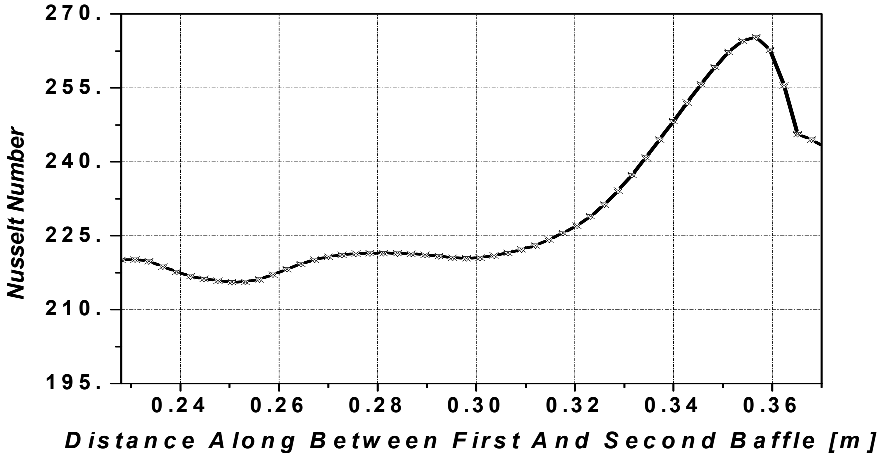

Figure 11. Local Nusselt number distribution between first and Second Baffle

5. CONCLUSION

A numerical analysis has been systematically performed for the turbulent fluid flow in horizontal channel containing two plate baffles in the lower and upper wall. The geometry of the problem is a simplification of the geometry found in shell-and tube heat exchangers. The computational methods based on k-ε model were applied. The numerical results show that the present numerical model suppressed the excessive production of turbulence energy near the impinging region and could reproduce complex turbulent flow characteristics with separation and reattachment around baffles. The recirculation above the roof of the baffle is moving downstream when the h becomes large. The higher perturbation is obtained for higher baffle dimensions.

The major conclusions are described as follows:

1. The rectangular baffle changes the incoming flow considerably resulting in recirculating zones on all surfaces of the baffle. The sizes and positions of these recirculating bubbles are tabulated and the effects of Re and wb/e on them are discussed.

2. The separating bubbles are responsible for the humps in the local Nusselt number variations along the baffle surfaces. The peak Nusselt number occurs near the point of reattachment.

3. Detailed comparison of the present prediction shows good agreement with experimental study of Demartini et al. (2004). The Deviation can be found near the recirculating bubble behind the baffle.

6. REFERENCES

Berner C, Durst F, McEligot DM., 1984, Flow around Baffles. ASME Journal of Heat Transfer.106:743-749.

Chen, C.H., Huang, W.H. ,1991,"Prediction for laminar forced convection in parallel-plate channels with transverse fin arrays", International Journal of Heat & Mass Transfer.34(11):

Demartini, L. C., Vielmo, H. A., and Möller, Q.V,2004, "Numeric and experimental analysis of turbulent flow through a channel with baffle plates", Journal of the Brazilian Society of Mechanical Sciences and Engineering. 26(2): 153-159.

Habib, M.A., Mobarak, A.M., Sallak, M.A., Abdel Hadi, E.A., Affify, R.I., 1994, "Experimental investigation of heat transfer and flow over baffles of different heights", Trans. ASME J. Heat Transfer. 116: 363–368.

Kelkar, K. M., Patankar, S. V, 1987, "Numerical prediction of flow and heat transfer in parallel plate channel with staggered fins", Journal of heat transfer, 109:25-30

Launder, B.E., Spalding, D. B. ,1974, "The numerical computation of turbulent flow", Computer Methods in Applied Mechanics and Engineering, 3: 269-289.

Patankar, S. V., 1980, "Numerical heat transfer and fluid flow", Series in Computational Methods in Mechanics and Thermal Sciences. Hemisphere Publ. Corp., McGraw-Hill

Roetzel, W., Lee, D. ,1993, "Experimental investigation of leakage in shell-and-tube heat exchangers with segmental ba.es", International Journal of Heat & Mass Transfer. 36:3765-3771.

Versteeg, H.K., and W., Malalasekera ,1995, "An introduction to Computational Fluid Dynamics. The finite volume method", Addison Wesley Longman Limited, England.

Webb, B.W., Ramadhyani, S., 1985, "Conjugate heat transfer in a channel with staggered ribs", International Journal of Heat & Mass Transfer,. 28:1679–1687.